Zanne, Amy E.; Flores-Moreno, Habacuc; Powell, Jeff; [et al.]. «Termite sensitivity to temperature affects global wood decay rates». Science, Vol. 377, no. 6613 (September 2022), p. 1440-1444. DOI 10.1126/science.abo3856

Termite sensitivity to temperature affects global wood decay rates

Authors: Amy E. Zanne[1*], Habacuc Flores-Moreno[2], Jeff R. Powell[3], William K. Cornwell[4], James W. Dalling[5], Amy T. Austin[6], Aimee T. Classen[7], Paul Eggleton[8], Kei-ichi Okada[9], Catherine L. Parr[10], E. Carol Adair[11], Stephen Adu-Bredu[12], Md Azharul Alam[13], Carolina Alvarez-Garzón[14], Deborah M.G. Apgaua[15], Roxana Aragón[16], Marcelo Ardón[17], Stefan K. Arndt[18], Louise A. Ashton[19], Nicholas A. Barber[20], Jacques Beauchene[21], Matty P. Berg[22], Jason Beringer[23], Matthias M. Boer[24], José Antonio Bonet[25], Katherine Bunney[26], Tynan J. Burkhardt[27], Dulcineia de Carvalho[28], Dennis Castillo-Figueroa[29], Lucas A. Cernusak[30], Alexander William Cheesman[31], Taina M. Cirne-Silva[32], Jamie Cleverly[33], Johannes H.C. Cornelissen[34], Timothy J. Curran[35], André Mouro D'Angioli[36], Caroline Dallstream[37], Nico Eisenhauer[38], Fidele Evouna Ondo[39], Alex Fajardo[40], Romina D. Fernandez[41], Astrid Ferrer[42], Marco Aurélio Leite Fontes[43], Mark L. Galatowitsch[44], Grizelle González[45], Felix Gottschall[46], Peter R. Grace[47], Elena Granda[48], Hannah M. Griffiths[49], Mariana Guerra Lara[50], Motohiro Hasegawa[51], Mariet M. Hefting [52], Nina Hinko-Najera[53], Lindsay B. Hutley[54], Jennifer M. Jones[55], Anja Kahl[56], Mirko Karan[57], Joost A. Keuskamp[58], Tim Lardner[59], Michael J. Liddell[60], Craig Macfarlane[61], Cate Macinnis-Ng[62], Ravi Fernandes Mariano[63], M. Soledad Méndez[64], Wayne S. Meyer[65], Akira S. Mori[66], Aloysio Souza de Moura[67], Matthew Northwood[68], Romà Ogaya[69], Rafael S. Oliveira[70], Alberto Orgiazzi[71], Juliana Pardo[72], Guille Peguero[73], Josep Penuelas[74], Luis Ignacio Perez[75], Juan Manuel Posada[76], Cecilia Margarita Prada[77], Tomáš Přívětivý[78], Suzanne M. Prober[79], Jonathan Prunier[80], Gabriel Willie Quansah[81], Víctor Resco de Dios[82], Ronny Richter[83], Mark Peter Robertson[84], Lucas Fernandes Rocha[85], Megan A. Rúa[86], Carolina Sarmiento[87], Richard P. Silberstein[88], Mateus Cardoso Silva[89], Flávia Freire Siqueira[90], Matthew Glenn Stillwagon[91], Jacqui Stol[92], Melanie K. Taylor[93], Francois Philippe Teste[94], David Yue Phin Tng[95], David Tucker[96], Manfred Türke[97], Michael D. Ulyshen[98], Oscar J. Valverde-Barrantes[99], Eduardo van den Berg[100], Richard S.P. van Logtestijn[101], G.F. (Ciska) Veen[102], Jason G. Vogel[103], Timothy J. Wardlaw[104], Georg Wiehl[105], Christian Wirth[106], Michaela J. Woods[107], Paul-Camilo Zalamea[108]

Affiliations:

[1]University of Miami; Miami, United States.

[2]University of Queensland; Brisbane, Australia.

[3]Western Sydney University; Richmond, Australia.

[4]University of New South Wales; Sydney, Australia.

[5]University of Illinois Urbana-Champaign; Urbana-Champaign, United States.

[6]Universidad de Buenos Aires; Buenos Aires, Argentina.

[7]University of Michigan; Ann Arbor, United States.

[8]The Natural History Museum, London; London, United Kingdom.

[9]Tokyo University of Agriculture; Tokyo, Japan.

[10]University of Liverpool; Liverpool, United Kingdom.

[11]University of Vermont; Burlington, United States.

[12]CSIR-Forestry Research Institute of Ghana; Kumasi, Ghana.

[13]Lincoln University; Lincoln, New Zealand.

[14]Universidad del Rosario; Bogotá, Colombia.

[15]School for Field Studies; Danbulla, Australia.

[16]Instituto de Ecología Regional (UNT-CONICET); Tucumán, Argentina.

[17]North Carolina State University; Raleigh, United States.

[18]The University of Melbourne; Melbourne, Australia.

[19]The University of Hong Kong; Hong Kong Special Administrative Region, China.

[20]San Diego State University; San Diego, United States.

[21]CIRAD; Paracou, French Guiana.

[22]Vrije Universiteit; Amsterdam, The Netherlands.

[23]University of Western Australia; Perth, Australia.

[24]Western Sydney University; Richmond, Australia.

[25]Joint Research Unit CTFC – AGROTECNIO – CERCA Center; Lleida, Spain.

[26]University of Pretoria; Pretoria, South Africa.

[27]University of Auckland; Auckland, New Zealand.

[28]Federal University of Lavras; Lavras, Brazil.

[29]Universidad del Rosario; Bogotá, Colombia.

[30]James Cook University; Cairns, Australia.

[31]James Cook University; Cairns, Australia.

[32]Federal University of Lavras; Lavras, Brazil.

[33]James Cook University; Cairns, Australia.

[34]Vrije Universiteit; Amsterdam, The Netherlands.

[35]Lincoln University; Lincoln, New Zealand.

[36]Universidade Estadual de Campinas; Campinas, Brazil.

[37]McGill University; Montréal, Canada.

[38]German Centre for Integrative Biodiversity Research; Leipzig, Germany.

[39]National Agency for National Parks; Libreville, Gabon.

[40]Universidad de Talca; Talca, Chile.

[41]Instituto de Ecología Regional (UNT-CONICET); Tucumán, Argentina.

[42]University of Illinois at Urbana-Champaign; Urbana-Champaign, United States.

[43]Federal University of Lavras; Lavras, Brazil.

[44]Centre College; Danville, United States.

[45]USDA Forest Service; San Juan, United States.

[46]German Centre for Integrative Biodiversity Research; Leipzig, Germany.

[47]Queensland University of Technology; Brisbane, Australia.

[48]Universidad de Alcalá; Alcalá de Henares, España.

[49]University of Bristol; Bristol, England.

[50]UNT-CONICET; Tucumán, Argentina.

[51]Doshisha University; Kyoto, Japan.

[52]Utrecht University; Utrecht, The Netherlands.

[53]The University of Melbourne; Creswick, Australia.

[54]Charles Darwin University; Darwin, Australia.

[55]University of Illinois Urbana-Champaign; Urbana-Champaign, United States.

[56]University of Leipzig; Leipzig, Germany.

[57]James Cook University; Cairns, Australia.

[58]Biont Research; Utrecht, The Netherlands.

[59]The University of Western Australia; Perth, Australia.

[60]James Cook University; Cairns, Australia.

[61]CSIRO Land and Water; Wembley, Australia.

[62]University of Auckland; Auckland, New Zealand.

[63]Federal University of Lavras; Lavras, Brazil.

[64]Universidad de Buenos Aires; Buenos Aires, Argentina.

[65]University of Adelaide; Adelaide, Australia.

[66]The University of Tokyo; Tokyo, Japan.

[67]Federal University of Lavras; Lavras, Brazil.

[68]Charles Darwin University; Darwin, Australia.

[69]CREAF-CSIC; Barcelona, Espanya.

[70]Universidade Estadual de Campinas; Campinas, Brazil.

[71]European Commission, Joint Research Centre; Ispra, Italy.

[72]Université de Montréal; Montréal, Canadá.

[73]Universitat Autònoma de Barcelona; Barcelona, Spain.

[74]CREAF-CSIC; Barcelona, Espanya.

[75]Universidad de Buenos Aires; Buenos Aires, Argentina.

[76]Universidad del Rosario; Bogotá, Colombia.

[77]University of Illinois Urbana-Champaign; Urbana-Champaign, United States.

[78]Silva Tarouca Research Institute for Landscape and Ornamental Gardening; Brno, Czechia.

[79]CSIRO Land and Water; Wembley, Australia.

[80]CNRS; Kourou, France.

[81]CSIR-Soil Research Institute; Kumasi, Ghana.

[82]University of Lleida; Lleda, Spain.

[83]German Centre for Integrative Biodiversity Research; Leipzig, Germany.

[84]University of Pretoria; Pretoria, South Africa.

[85]Federal University of Lavras; Lavras, Brazil.

[86]Wright State University; Dayton, United States.

[87]University of South Florida; Tampa, United States.

[88]Edith Cowan University; Joondalup, Australia.

[89]Federal University of Lavras; Lavras, Brazil.

[90]Federal University of Lavras; Lavras, Brazil.

[91]North Carolina State University; Raleigh, United States.

[92]CSIRO; Canberra, Australia.

[93]USDA Forest Service; Athens, United States.

[94]IMASL-CONICET and Universidad Nacional de San Luis; San Luis, Argentina.

[95]The School for Field Studies; Danbulla, Australia.

[96]Queensland University of Technology; Brisbane, Australia.

[97]German Centre for Integrative Biodiversity Research; Leipzig, Germany.

[98]USDA Forest Service; Athens, United States.

[99]Florida International University; Miami, United States.

[100]Federal University of Lavras; Lavras, Brazil.

[101]Vrije Universiteit; Amsterdam, The Netherlands.

[102]NIOO-KNAW; Wageningen, Netherlands.

[103]University of Florida; Gainesville, United States.

[104]University of Tasmania; Hobart, Australia.

[105]CSIRO Land and Water; Wembley, Australia.

[106]Leipzig University; Leipzig, Germany.

[107]University of Dayton; Dayton, United States.

[108]University of South Florida; Tampa, United States.

*Corresponding author. Email: aezanne@gmail.com

Abstract: Deadwood is a large global carbon store with its store size partially determined by biotic decay. Microbial wood decay rates are known to respond to changing temperature and precipitation. Termites are also important decomposers in the tropics but are less well studied. An understanding of their climate sensitivities is needed to estimate climate change effects on wood carbon pools. Using data from 133 sites spanning six continents, we found that termite wood discovery and consumption were highly sensitive to temperature (with decay increasing >6.8 times per 10°C increase in temperature)—even more so than microbes. Termite decay effects were greatest in tropical seasonal forests, tropical savannas, and subtropical deserts. With tropicalization (i.e., warming shifts to tropical climates), termite wood decay will likely increase as termites access more of Earth's surface.

One-Sentence Summary: Termites respond to temperature much more strongly than microbes,changing our view of wood decay and the carbon cycle.

Main Text:

Forests contain ~676 Gt of biomass (*1*), with a large fraction of their carbon immobilized for centuries in living and deadwood (*2*, *3*). Carbon storage depends partly on decay rates of deadwood pools by organisms, which vary across climatic gradients (*4*, *5*). Regional studies suggest wood decay by microbes approximately doubles with a 10°C temperature increase (decay effective Q_{10} = ~2) (*2*, *6*) driven, in part, by enzyme kinetics. Further, microbial decay occurs via extracellular enzymes whose delivery is dependent on moisture (*7*, *8*), meaning microbial decay should increase with humidity. Less is known about the climate sensitivities of important animal decayers, which also influence how climate change affects deadwood carbon stores.

Increasing evidence shows that termites are important decayers at local to regional scales (*7*, *9*, *10*). The abundance of wood-feeding termites across biomes is poorly understood (*11*), but decay by termites should be temperature sensitive. First, termites increasingly contribute to wood decay in warm locations (*12*–*14*), with distributions set in part by ectothermic temperature tolerances (*15*). Termite wood decay depends on both discovery and consumption of wood by searching animals, followed by chemical decay via a cultivated set of microbial symbionts. Therefore, second, this symbiont chemical decay will also be shaped by temperature-dependent enzyme kinetics. For moisture, in contrast to microbes, termites have a diversity of adaptations to conserve it that presumably buffer their sensitivities to low precipitation (*16*–*18*), meaning termite discovery and decay likely continues with increasing aridity.

To test climate sensitivities of termite and microbial decay, we conducted a replicated wood decay experiment at 133 sites across extensive temperature and precipitation gradients representing most of the global bioregions (Fig. 1). At each site, researchers monitored decay of wood blocks for a common substrate, *Pinus radiata* (or in a few cases closely related *Pinus* species; see (*19*)), for up to 48 months. All sites had harvests at ~12 months and most at ~24 months with some sites including ~6 month, ~36 month and/or ~48 month harvests. We allowed microbial access to all samples and manipulated termite access ("microbes" versus "microbes+termites" treatments); wood blocks were wrapped in fine mesh with or without larger holes to allow or exclude termites. At each site, researchers placed pairs of treatment blocks with number of pairs equal to number of harvests planned at each of 20 stations (a few sites placed fewer stations), meaning each harvest from a site had 40 wood blocks (mean = 33.6 $\pm$ 14.2 (1SD)) harvested at a given time point across both treatments; stations were spaced at least 5 m apart (see (*19*), table S11). A total of 8,922 blocks were collected across all sites. Our focal species, *P. radiata*, was non-native at all locations, meaning no site decay agents evolved with it as a substrate.

Termite discovery, estimated percentage of wood blocks with evidence of termites per year at a site, was greatest, but also highly variable, at low latitudes and elevations and where temperature and precipitation were high (Fig. 1A, B, fig. S1; table S1). High wood block discovery (>50%) occurred at temperatures above 21.3°C. In multivariate models, wood block discovery by termites rapidly increased with increasing temperatures (Fig. 2A, table S3) and temperature and precipitation significantly interacted (Figs 1B, 2A, table S3). Termite discovery was higher in warm tropical biomes in arid and semi-arid sites (despite small sample sizes) than in mesic and humid sites (at 25°C, discovery estimates at 250 mm were 1.4× higher than at 2000 mm and 1.9× higher than at 2700 mm), while in cool temperate biomes the reverse patterns were observed (at 7°C, discovery estimates at 2700 mm were 4× higher than at 2000 mm and 150× higher than at 250 mm).

Microbial decay was fastest at low latitudes and elevations and where temperature and precipitation were high, although latitude and precipitation were weaker predictors than elevation and temperature (Fig. 1C, fig. S2; table S2). Microbial temperature sensitivity was similar to regional studies (decay effective Q_{10} of 1.73; 95% CI: 1.45-2.09) (*2*, *6*). In multivariate models, precipitation was not a significant predictor of microbial decay (Fig. 2B, table S4). When termites discovered wood, decay rates were higher at low elevations and where temperature was high (Fig. 1C, fig. S2; table S2). Further, decay rates in termite discovered wood were more sensitive to changes in temperature (decay effective Q_{10} of 6.85; 95% CI: 4.73-9.92) than decay rates in undiscovered wood where microbes dominated decay. In multivariate models, precipitation was not a significant predictor of decay for termite discovered wood (Fig. 2C, table S5).

The termite-discovered wood decay effective Q_{10} is much steeper than any previously recorded for microbes (*2*, *6*), suggesting that a different mechanism determines termite versus microbial decay. The observed high consumption rate by termites at warm sites may be related to termite assemblage composition, large population numbers, high activity or some combination of these mechanisms and implies that residence times of wood may be much shorter than expected due to termites in warm locations. Consequently, subtropical, tropical or global models using a single microbial-derived decay effective Q_{10} are likely to: (1) underpredict wood decay; (2) overpredict terrestrial carbon storage (all else being equal, e.g., inputs into deadwood pools); and (3) underpredict temperature sensitivity of decay. Use of termite-corrected decay effective Q_{10}s, which may vary based on termite assemblage composition, location and/or wood substrate, should improve accuracy of modeled wood decay under current and future climate predictions. Such model modifications can capitalize on empirical measures in the literature such as ours for termites and (*20*) for insects more broadly. Our results suggest precipitation variation influences the discovery, but not decay phase, of termite wood decay. However, strong temperature and precipitation interaction influences on discovery mean that termites increased overall decay most in subtropical deserts and tropical seasonal forests and savannas(Fig. 1C). Further, even though microbial abundance is sensitive to precipitation (*4*, *5*), temperature was a stronger driver than precipitation for microbial-driven decay, perhaps mediated through effects on enzyme kinetics (*21*). Differences in decay sensitivity to precipitation were small with only microbial-mediated wood decay weakly sensitive to precipitation; microbial decay largely occurs via release of moisture-sensitive extracellular enzymes (*7*, *8*), while termites can conserve moisture, buffering aridity effects (*16*–*18*). While low termite discovery in warm humid locations remains surprising, competitive interactions between decayers (*11*, *13*), biome-specific adaptations to moisture, variation in resource availability affecting foraging behavior, etc., may reduce discovery.

Given extreme sensitivities of both termite wood discovery and decay to temperature, termites will likely expand their range in a warming world with important consequences for carbon cycling. Using data-driven estimates of temperature and precipitation effects on termite discovery (Table S3), we estimated discovery rates across the globe, restricting predictions to the range in MAP covered by our sites $\pm$10%. Termites today have potential to discover large amounts of deadwood (>50%) at sites across 30.2% of the land surface (assuming our estimated discovery rates apply across wood and termite species; Fig. 3). To bracket potential climate change effects on discovery, we used our estimated climate relationships with all available midcentury CMIP6 climate models for SSP 1-2.6 and 5-8.5 (*22*). All scenarios predicted an expansion of termite discovery in tropical and subtropical regions with the degree of expansion depending strongly on extent of global warming (Fig. 3). Warming shifts to more tropical climates are occurring in many ecosystems globally (*23*), and temperature sensitivities demonstrated in this study suggest termite contributions to wood decay will expand both within and beyond the tropics with such tropicalization. Our estimates may even underpredict termite effects in areas where fungus-growing termites occur (i.e., Africa and Asia) (*12*, *16*), meriting future focus. The impact of termites on wood decay is both large and expected to increase (Fig. 3); it also has a different functional form than microbial decay with a clear two-step process: discovery and decay.

References and Notes

1. G. Kindermann, I. McCallum, S. Fritz, M. Obersteiner, A global forest growing stock, biomass and carbon map based on FAO statistics. *Silva Fenn.* **42**, 387–396 (2008).
2. M. E. Harmon, B. G. Fasth, M. Yatskov, D. Kastendick, J. Rock, C. W. Woodall, Release of coarse woody detritus-related carbon: a synthesis across forest biomes. *Carbon Balance Manag.* **15**, 1 (2020).
3. J. Mackensen, J. Bauhus, Density loss and respiration rates in coarse woody debris of *Pinus radiata, Eucalyptus regnans* and *Eucalyptus maculata. Soil Biol. Biochem.* **35**, 177–186 (2003).
4. A. T. Austin, P. M. Vitousek, Precipitation, decomposition and litter decomposability of *Metrosideros polymorpha* in native forests on Hawai'i. *J. Ecol.* **88**, 129–138 (2000).
5. B. N. Marais, C. Brischke, H. Militz, J. H. Peters, L. Reinhardt, Studies into Fungal Decay of Wood In Ground Contact—Part 1: The Influence of Water-Holding Capacity, Moisture Content, and Temperature of Soil Substrates on Fungal Decay of Selected Timbers. *Forests*. **11**, 1284 (2020).

6. N. Fierer, B. P. Colman, J. P. Schimel, R. B. Jackson, Predicting the temperature dependence of microbial respiration in soil: A continental-scale analysis. *Glob. Biogeochem. Cycles*. **20** (2006), doi:10.1029/2005GB002644.

7. W. K. Cornwell, J. H. C. Cornelissen, S. D. Allison, J. Bauhus, P. Eggleton, C. M. Preston, F. Scarff, J. T. Weedon, C. Wirth, A. E. Zanne, Plant traits and wood fates across the globe: rotted, burned, or consumed? *Glob. Change Biol.* **15**, 2431–2449 (2009).

8. A. D. A'Bear, T. H. Jones, E. Kandeler, L. Boddy, Interactive effects of temperature and soil moisture on fungal-mediated wood decomposition and extracellular enzyme activity. *Soil Biol. Biochem.* **70**, 151–158 (2014).

9. M. D. Ulyshen, Wood decomposition as influenced by invertebrates. *Biol. Rev. Camb. Philos. Soc.* **91**, 70–85 (2016).

10. H. M. Griffiths, L. A. Ashton, C. L. Parr, P. Eggleton, The impact of invertebrate decomposers on plants and soil. *New Phytol.* **231**, 2142–2149 (2021).

11. R. A. Clement, H. Flores-Moreno, L. A. Cernusak, A. W. Cheesman, A. R. Yatsko, S. D. Allison, P. Eggleton, A. E. Zanne, Assessing the Australian Termite Diversity Anomaly: How Habitat and Rainfall Affect Termite Assemblages. *Front. Ecol. Evol.* **9**, 237 (2021).

12. H. M. Griffiths, L. A. Ashton, T. A. Evans, C. L. Parr, P. Eggleton, Termites can decompose more than half of deadwood in tropical rainforest. *Curr. Biol.* **29**, R118–R119 (2019).

13. M. A. Bradford, D. S. Maynard, T. W. Crowther, P. T. Frankson, J. E. Mohan, C. Steinrueck, G. F. (Ciska) Veen, J. R. King, R. J. Warren II, Belowground community turnover accelerates the decomposition of standing dead wood. *Ecology*. **102**, e03484 (2021).

14. C. Guo, B. Tuo, H. Ci, E.-R. Yan, J. H. C. Cornelissen, Dynamic feedbacks among tree functional traits, termite populations and deadwood turnover. *J. Ecol.* **109**, 1578–1590 (2021).

15. O. F. Palin, P. Eggleton, Y. Malhi, C. A. J. Girardin, A. Rozas-Dávila, C. L. Parr, Termite Diversity along an Amazon–Andes Elevation Gradient, Peru. *Biotropica*. **43**, 100–107 (2011).

16. J. A. Bonachela, R. M. Pringle, E. Sheffer, T. C. Coverdale, J. A. Guyton, K. K. Caylor, S. A. Levin, C. E. Tarnita, Termite mounds can increase the robustness of dryland ecosystems to climatic change. *Science* (2015), doi:10.1126/science.1261487.

17. L. A. Ashton, H. M. Griffiths, C. L. Parr, T. A. Evans, R. K. Didham, F. Hasan, Y. A. Teh, H. S. Tin, C. S. Vairappan, P. Eggleton, Termites mitigate the effects of drought in tropical rainforest. *Science*. **363**, 174–177 (2019).

18. A. W. Cheesman, L. A. Cernusak, A. E. Zanne, Relative roles of termites and saprotrophic microbes as drivers of wood decay: A wood block test. *Austral Ecol.* **43**, 257–267 (2018).

19. Materials and methods are available as supplementary materials.

20. S. Seibold, W. Rammer, T. Hothorn, R. Seidl, M. D. Ulyshen, J. Lorz, M. W. Cadotte, D. B. Lindenmayer, Y. P. Adhikari, R. Aragón, S. Bae, P. Baldrian, H. Barimani Varandi, J. Barlow, C. Bässler, J. Beauchêne, E. Berenguer, R. S. Bergamin, T. Birkemoe, G. Boros, R. Brandl, H. Brustel, P. J. Burton, Y. T. Cakpo-Tossou, J. Castro, E. Cateau, T. P. Cobb, N. Farwig, R. D. Fernández, J. Firn, K. S. Gan, G. González, M. M. Gossner, J. C. Habel, C. Hébert, C. Heibl, O. Heikkala, A. Hemp, C. Hemp, J. Hjältén, S. Hotes, J. Kouki, T. Lachat, J. Liu, Y. Liu, Y.-H. Luo, D. M. Macandog, P. E. Martina, S. A. Mukul, B. Nachin, K. Nisbet, J. O'Halloran, A. Oxbrough, J. N. Pandey, T. Pavlíček, S. M. Pawson, J. S.

Rakotondranary, J.-B. Ramanamanjato, L. Rossi, J. Schmidl, M. Schulze, S. Seaton, M. J. Stone, N. E. Stork, B. Suran, A. Sverdrup-Thygeson, S. Thorn, G. Thyagarajan, T. J. Wardlaw, W. W. Weisser, S. Yoon, N. Zhang, J. Müller, The contribution of insects to global forest deadwood decomposition. *Nature*. **597**, 77–81 (2021).

21. G. Wang, W. M. Post, M. A. Mayes, Development of microbial-enzyme-mediated decomposition model parameters through steady-state and dynamic analyses. *Ecol. Appl.* **23**, 255–272 (2013).

22. V. Eyring, S. Bony, G. A. Meehl, C. A. Senior, B. Stevens, R. J. Stouffer, K. E. Taylor, Overview of the Coupled Model Intercomparison Project Phase 6 (CMIP6) experimental design and organization. *Geosci. Model Dev.* **9**, 1937–1958 (2016).

23. A. Vergés, P. D. Steinberg, M. E. Hay, A. G. B. Poore, A. H. Campbell, E. Ballesteros, K. L. Heck, D. J. Booth, M. A. Coleman, D. A. Feary, W. Figueira, T. Langlois, E. M. Marzinelli, T. Mizerek, P. J. Mumby, Y. Nakamura, M. Roughan, E. van Sebille, A. S. Gupta, D. A. Smale, F. Tomas, T. Wernberg, S. K. Wilson, The tropicalization of temperate marine ecosystems: climate-mediated changes in herbivory and community phase shifts. *Proc. R. Soc. B Biol. Sci.* **281**, 20140846 (2014).

24. R. E. Ricklefs, *The Economy of Nature* (Macmillan, 2008).

25. J. T. Weedon, W. K. Cornwell, J. H. C. Cornelissen, A. E. Zanne, C. Wirth, D. A. Coomes, Global meta-analysis of wood decomposition rates: a role for trait variation among tree species? *Ecol. Lett.* **12**, 45–56 (2009).

26. B. Oberle, M. R. Lee, J. A. Myers, O. L. Osazuwa-Peters, M. J. Spasojevic, M. L. Walton, D. F. Young, A. E. Zanne, Accurate forest projections require long-term wood decay experiments because plant trait effects change through time. *Glob. Change Biol.* **26**, 864–

875 (2020).

27. S. E. Fick, R. J. Hijmans, WorldClim 2: new 1-km spatial resolution climate surfaces for global land areas. *Int. J. Climatol.* **37**, 4302–4315 (2017).

28. R. J. Hijmans, J. van Etten, M. Sumner, J. Cheng, D. Baston, A. Bevan, R. Bivand, L. Busetto, M. Canty, B. Fasoli, D. Forrest, A. Ghosh, D. Golicher, J. Gray, J. A. Greenberg, P. Hiemstra, K. Hingee, A. Ilich, I. for M. A. Geosciences, C. Karney, M. Mattiuzzi, S. Mosher, B. Naimi, J. Nowosad, E. Pebesma, O. P. Lamigueiro, E. B. Racine, B. Rowlingson, A. Shortridge, B. Venables, R. Wueest, raster: Geographic Data Analysis and Modeling (2022), (available at https://CRAN.R-project.org/package=raster).

29. V. Ștefan, plotbiomes (2021), (available at https://github.com/valentinitnelav/plotbiomes).

30. R Core Team, R: A language and environment for statistical computing. R Foundation for Statistical Computing, Vienna, Austria. URL https://www.R-project.org/. (2021).

31. V. Spinu, G. Grolemund, H. Wickham, D. Vaughan, I. Lyttle, I. Costigan, J. Law, D. Mitarotonda, J. Larmarange, J. Boiser, C. H. Lee, G. Inc, lubridate: Make Dealing with Dates a Little Easier (2021), (available at https://CRAN.R-project.org/package=lubridate).

32. A. Canty, B. Ripley, boot: Bootstrap Functions (Originally by Angelo Canty for S) (2021), (available at https://CRAN.R-project.org/package=boot).

33. D. Makowski, D. Lüdecke, M. S. Ben-Shachar, I. Patil, B. M. Wiernik, R. Siegel, report: Automated Reporting of Results and Statistical Models (2022), (available at https://CRAN.R-project.org/package=report).

34. D. Lüdecke, D. Makowski, I. Patil, M. S. Ben-Shachar, B. M. Wiernik, P. Waggoner, J. R. Stevens, M. Smith, J. Bossek, see: Visualisation Toolbox for “easystats” and Extra Geoms, Themes and Color Palettes for “ggplot2” (2022), (available at https://CRAN.R-

project.org/package=see).

35. D. Makowski, B. M. Wiernik, I. Patil, D. Lüdecke, M. S. Ben-Shachar, M. White, M. M. Rabe, correlation: Methods for Correlation Analysis (2022), (available at https://CRAN.R-project.org/package=correlation).

36. D. Makowski, D. Lüdecke, M. S. Ben-Shachar, I. Patil, modelbased: Estimation of Model-Based Predictions, Contrasts and Means (2022), (available at https://CRAN.R-project.org/package=modelbased).

37. M. S. Ben-Shachar, D. Makowski, D. Lüdecke, I. Patil, B. M. Wiernik, K. Kelley, D. Stanley, J. Burnett, J. Karreth, effectsize: Indices of Effect Size and Standardized Parameters (2022), (available at https://CRAN.R-project.org/package=effectsize).

38. D. Lüdecke, D. Makowski, M. S. Ben-Shachar, I. Patil, S. Højsgaard, B. M. Wiernik, Z. J. Lau, V. Arel-Bundock, J. Girard, C. Maimone, N. Ohlsen, D. E. Morrison, parameters: Processing of Model Parameters (2022), (available at https://CRAN.R-project.org/package=parameters).

39. D. Lüdecke, D. Makowski, M. S. Ben-Shachar, I. Patil, P. Waggoner, B. M. Wiernik, V. Arel-Bundock, M. Jullum, performance: Assessment of Regression Models Performance (2022), (available at https://CRAN.R-project.org/package=performance).

40. D. Makowski, D. Lüdecke, M. S. Ben-Shachar, I. Patil, M. D. Wilson, B. M. Wiernik, P.-C. Bürkner, T. Mahr, H. Singmann, Q. F. Gronau, S. Crawley, bayestestR: Understand and Describe Bayesian Models and Posterior Distributions (2022), (available at https://CRAN.R-project.org/package=bayestestR).

41. D. Makowski, D. Lüdecke, I. Patil, M. S. Ben-Shachar, B. M. Wiernik, E. Bacher, datawizard: Easy Data Wrangling (2022), (available at https://CRAN.R-

project.org/package=datawizard).

42. D. Lüdecke, D. Makowski, I. Patil, P. Waggoner, M. S. Ben-Shachar, B. M. Wiernik, V. Arel-Bundock, A. Hayes, insight: Easy Access to Model Information for Various Model Objects (2022), (available at https://CRAN.R-project.org/package=insight).
43. easystats/easystats: The R easystats-project, (available at https://github.com/easystats/easystats).
44. D. Bates, M. Maechler, B. Bolker [aut, S. Walker, R. H. B. Christensen, H. Singmann, B. Dai, F. Scheipl, G. Grothendieck, P. Green, J. Fox, A. Bauer, P. N. Krivitsky, lme4: Linear Mixed-Effects Models using "Eigen" and S4 (2022), (available at https://CRAN.R-project.org/package=lme4).
45. T. L. Pedersen, patchwork: The Composer of Plots (2020), (available at https://CRAN.R-project.org/package=patchwork).
46. D. Lüdecke, F. Aust, S. Crawley, M. S. Ben-Shachar, ggeffects: Create Tidy Data Frames of Marginal Effects for "ggplot" from Model Outputs (2022), (available at https://CRAN.R-project.org/package=ggeffects).
47. H. Wickham, forcats: Tools for Working with Categorical Variables (Factors) (2021), (available at https://CRAN.R-project.org/package=forcats).
48. H. Wickham, stringr: Simple, Consistent Wrappers for Common String Operations (2019), (available at https://CRAN.R-project.org/package=stringr).
49. H. Wickham, R. François, L. Henry, K. Müller, dplyr: A Grammar of Data Manipulation (2022), (available at https://CRAN.R-project.org/package=dplyr).
50. L. Henry, H. Wickham, purrr: Functional Programming Tools (2020), (available at https://CRAN.R-project.org/package=purrr).

51. H. Wickham, J. Hester, R. Francois, J. Bryan, S. Bearrows, J. Jylänki, M. Jørgensen, readr: Read Rectangular Text Data (2022), (available at https://CRAN.R-project.org/package=readr).
52. H. Wickham, M. Girlich, tidyr: Tidy Messy Data (2022), (available at https://CRAN.R-project.org/package=tidyr).
53. K. Müller, H. Wickham, R. Francois, J. Bryan, tibble: Simple Data Frames (2022), (available at https://CRAN.R-project.org/package=tibble).
54. H. Wickham, W. Chang, L. Henry, T. L. Pedersen, K. Takahashi, C. Wilke, K. Woo, H. Yutani, D. Dunnington, ggplot2: Create Elegant Data Visualisations Using the Grammar of Graphics (2022), (available at https://CRAN.R-project.org/package=ggplot2).
55. H. Wickham, tidyverse: Easily Install and Load the "Tidyverse" (2021), (available at https://CRAN.R-project.org/package=tidyverse).
56. N. Frerebeau, B. Lebrun, V. Arel-Bundock, khroma: Colour Schemes for Scientific Data Visualization (2019), (available at https://hal.archives-ouvertes.fr/hal-01927931).
57. J. Fox, S. Weisberg, *An R Companion to Applied Regression* (Sage, Thousand Oaks, CA, Third., 2019; https://us.sagepub.com/en-us/nam/an-r-companion-to-applied-regression/book246125).

Acknowledgments: For materials, field, and lab assistance, we thank the Australian Landscape Trust Team, Juan Martínez de Aragón, Eric Roy, Hugh Wilson, Kylie Brice, Bethanie Coleman, Brendan Delroy, Coline Deveautour, Suzanne Donn, Generci Assis Neves, Ricardo Marques Barreiros, Ricardo Marques Barreiros, Generci Assis Neves from Resineves Agroflorestal company, Alfred Lochner, Pousada Vale do Céu, Humberto Robles, María M. Rivera, and Grant Kirker. We also thank the World Climate Research Programme for producing and making available their model output, the Earth System Grid Federation (ESGF) for archiving the data and providing access, and the multiple funding agencies who support CMIP6 and ESGF. Steve Allison, Tom Crowther and three anonymous reviewers provided helpful comments on the manuscript, and Abbey Yatsko helped with figure and manuscript formatting.

Funding:

US National Science Foundation DEB-1655759, (AEZ)

US National Science Foundation DEB-2149151 (AEZ)

US National Science Foundation DEB-1713502 (MA)

US National Science Foundation DEB-1713435 (MA)

US National Science Foundation DEB-1647502 (NAB)

US National Science Foundation DEB-1546686 (GG)

US National Science Foundation DEB-1831952 (GG)

George Washington University (AEZ)

USDA Forest Service (GG)

Centre College Faculty Development Funds (MLG)

Australia Terrestrial Ecosystem Research Network National Collaborative Research Infrastructure Strategy (PRG, JC, MK, MJL, MMB, RPS, JS, LH, MN, SMP, TJW, SKA)

Royal Society-FCDO Africa Capacity Building Initiative (CLP, GWQ, SAB, KB)

New Phytologist Foundation (ATA)

Fondecyt grant 1160329 (CD)

Coordenação de Aperfeiçoamento de Pessoal de Nível Superior, Brasil (CAPES) (EVDB, ASM, RFM, SFF, TMCS)

Department of Ecology and Conservation of the Federal University of Lavras (TMCS)

CNPq (EVDB)

FAPEMIG (EVDB)

Australian Academy of Science 2017 Thomas Davies Research Grant (JRP)

Australian Research Council DP160103765 (JRP)

UK National Environment Research Council NE/L000016/1 (LAA)

Fundação de Amparo à Pesquisa do Estado de São Paulo, Brazil NERC - FAPESP 19/07773-1 (RSO, AMD)

Environment Research and Technology Development Fund ERTDF, JPMEERF15S11420 of the Environmental Restoration and Conservation Agency of Japan (ASM, KO)

COLCIENCIAS No. FP44842-046-2017 (JMP)

Spanish Government PID2019-110521GB-I00 (JP, GP, RO)

Catalan Government grant SGR 2017-1005 (JP, GP, RO)

Fundación Ramón Areces ELEMENTAL-CLIMATE (JP, GP, RO)

Consejo Nacional de Investigaciones Científicas y Técnicas (LIP)

Agencia Nacional de Promoción Científica y Tecnológica PICT 2019- 2472 (LIP)

National Agency for the Promotion of Research, Technological Development and Innovation, Scientific and Technological Research Project 2018-01561 PICT 2018-01561 (FPT)

iDiv German Research Foundation DFG– FZT 118, 202548816 (NE)

European Research Council Horizon 2020 research and innovation program no. 677232 (NE)

Author contributions:

Conceptualization: AEZ

Methodology: AEZ, AWC, LAC, MK, JWD

Investigation: AEZ, AWC, LAC, MK, JRP, JWD, ATA, ATC, PE, KO, CLP, ECA, SAB, MA, CAG, DMGA, RA, MA, SKA, LAA, NAB, JB, MPB, JBer, MMB, JAB, KB, TJB, DC, DCF, LAC, AWC, TMCS, JC, JHC, TJC, AMD, CD, NE, FEO, AF, RDF, AFe, MALF, MLG, GG, FG, PRG, EG, HMG, MGL, MH, MMH, NH, LH, JMJ, AK, MK, JAK, TDL, MJL, CM, CMN, RFM, MSM, WSM, ASM, ASDM, MN, RO, RSO, AO, MJP, GP, JP, LIP, JMP, CMP, TP, SMP, JPr, GWQ, VRD, RR, MPR, LFR, MAR, CS, RPS, MCS, FFS, MGS, JS, MKT, FPT, DYPT, DT, MT, MDU, OVB, EVDB, RSPL, GFV, JGV, TJW, GW, CW, MJW, PCZ

Visualization: HFM, JRP, WKC

Funding acquisition: AEZ, AWC, LAC, MK, JRP, JWD, ATA, ATC, PE, KO, CLP, ECA, SAB, MA, CAG, DMGA, RA, MA, SKA, LAA, NAB, JB, MPB, JBer, MMB, JAB, KB, TJB, DC, DCF, LAC, AWC, TMCS, JC, JHC, TJC, AMD, CD, NE, FEO, AF, RDF, AFe, MALF, MLG, GG, FG, PRG, EG, HMG, MGL, MH, MMH, NH, LH, JMJ, AK, MK, JAK, TDL, MJL, CM, CMN, RFM, MSM, WSM, ASM, ASDM, MN, RO, RSO, AO, MJP, GP, JP, LIP, JMP, CMP, TP, SMP, JPr, GWQ, VRD, RR, MPR, LFR, MAR, CS, RPS, MCS, FFS, MGS, JS, MKT, FPT, DYPT, DT, MT, MDU, OVB, EVDB, RSPL, GFV, JGV, TJW, GW, CW, MJW, PCZ

Project administration: AEZ

Supervision: AEZ

Writing – original draft: AEZ, HFM, JRP, WKC, JWD, ATA, ATC

Writing – review & editing: AWC, LAC, MK, ATA, ATC, PE, KO, CLP, ECA, SAB, MA, CAG, DMGA, RA, MA, SKA, LAA, NAB, JB, MPB, JBer, MMB, JAB, KB, TJB, DC, DCF, LAC, AWC, TMCS, JC, JHC, TJC, AMD, CD, NE, FEO, AF, RDF, AFe, MALF, MLG, GG, FG, PRG, EG, HMG, MGL, MH, MMH, NH, LH, JMJ, AK, MK, JAK, TDL, MJL, CM, CMN, RFM, MSM, WSM, ASM, ASDM, MN, RO, RSO, AO, MJP, GP, JP, LIP, JMP, CMP, TP, SMP, JPr, GWQ, VRD, RR, MPR, LFR, MAR, CS, RPS, MCS, FFS, MGS, JS, MKT, FPT, DYPT, DT, MT, MDU, OVB, EVDB, RSPL, GFV, JGV, TJW, GW, CW, MJW, PCZ

Competing interests: Authors declare that they have no competing interests.

Data and materials availability: Data are available at https://doi.org/10.6084/m9.figshare.19920416.v1 and code are available at https://doi.org/10.5281/zenodo.6804781 .

Supplementary Materials

Materials and Methods

Figs. S1 to S4

Tables S1 to S12

References (*25*-*57*)

Figure Legends:

Fig. 1. Geographic, biome and climatic distribution of experimental sites. (**A**) Dots denote the 133 study site locations. (**B**) Study site distribution across mean annual temperatures (MAT), mean annual precipitations (MAP) and Whittaker biomes. In (**A**) and (**B**), color of the dots represents termite discovery rate (i.e., estimated percentage of wood blocks with evidence of

termites per year at a site). (**C**) Decay rate (k) estimates across Whittaker (*24*) biomes (shown by arrows and colors matching legend in (**B**), with boxplots for each biome representing blocks discovered by termites (dashed boxplots on right of pair) and blocks undiscovered by termites (solid boxplots on left of pair; examples of discovered blocks in fig. S3). Note that the y-axis is ln-transformed but tick labels represent untransformed values for decay. For boxplots, center line, median; box limits, upper and lower quartiles; whiskers, 1.5× interquartile range; points, outliers. Numbers on top of solid boxplots on left of pair indicate total number of sites per biome; numbers on top of dashed box plots on right of pair indicate number of sites where termite discovery occurred.

Fig. 2. Discovery and decay of wood based on significant (tables S3-5**) climatic predictors.** **(A**) Termite discovery rate, the estimated percentage of wood blocks in the microbes+termites treatment across all sites with evidence of termites per year across mean annual temperature (MAT) and mean annual precipitation (MAP), (**B**) Decay rates (k) of termite undiscovered wood across MAT, and (**C**) Decay rates (k) of termite discovered wood across MAT (Note: MAP was not a significant predictor of termite undiscovered or discovered wood). Symbols in figures denote role of wood-feeding termites  and/or wood-dwelling microbes . Solid lines represent logistic (for **A**) or linear (for **B** and **C**) regression predictions at 250 mm MAP (orange; representative of mean desert/savanna biomes), 2000 mm MAP (cream; representative of mean temperate biomes) and 2700 mm MAP (blue; representative of mean tropical/temperate humid biomes). Dashed lines represent 95% confidence intervals around predictions. The y-axes for **B** and **C** are ln-transformed but tick labels represent untransformed values for decay.

Fig. 3. Predicted termite discovery by mid-century under different tropicalization scenarios. Global maps showing minimum and maximum termite expansions scenarios based on the model in Table S3 and CMIP6 forecasts for 2041-2060. (**A**) Stronger climate change scenarios (SSP 5-8.5 UKESM1-0-LL) had the largest expansion in discovery rates and (**B**) weaker climate change scenarios (SSP 1-2.6 MPI-ESM1-2-HR) had the smallest. For (**A**) and (**B**), termite discovery categories were rare (<5% = grey), continuing low (<50% = bright green), current high (>50% = olive green), midcentury expansion to high (>50% = yellow) and unable to predict, restricting predictions to the range in MAP covered by our sites (± 10%). We did not model the transitions from rare (<5%; grey) to continuing low (>5% & <50%; bright green) discovery. Panel (**C**) shows forecast increases in terrestrial area (km^2) with discovery >50% by midcentury versus forecast mean terrestrial warming relative to a historical baseline. Each point denotes a forecast based on one individual CMIP6 SSP 5-8.5 or SSP 1-2.6 climate model. The x-axis of panel (**C**) is the mean forecast 2041-2060 warming above the 1970-2000 baseline for terrestrial areas only.

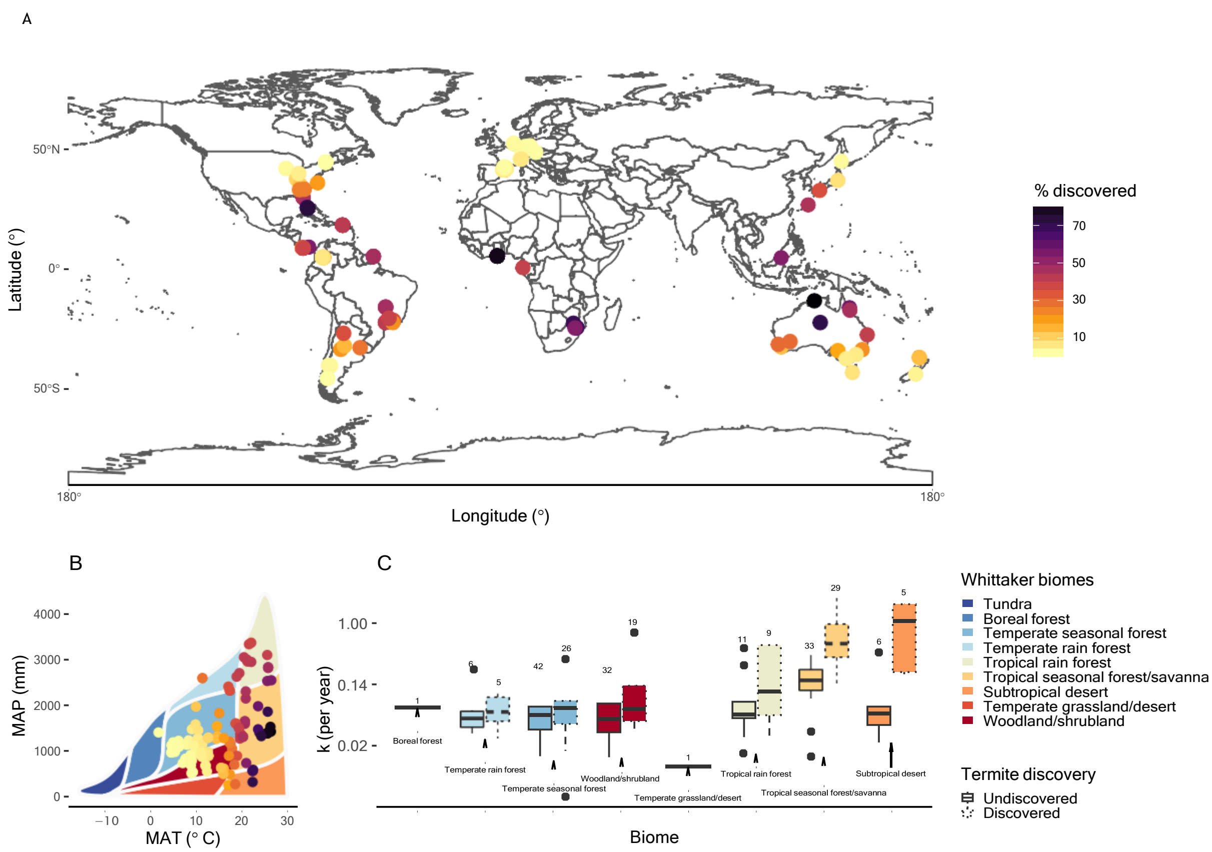
A
50°N
0°
50°S
Latitude (°)
180°
180°
Longitude (°)
% discovered
70
50
30
10
B
4000
3000
2000
1000
0
MAP (mm)
−10
0
10
20
30
MAT (° C)
C
1.00
0.14
0.02
k (per year)
Boreal forest
Temperate rain forest
Temperate seasonal forest
Woodland/shrubland
Temperate grassland/desert
Tropical rain forest
Tropical seasonal forest/savanna
Subtropical desert
Biome
Whittaker biomes
Tundra
Boreal forest
Temperate seasonal forest
Temperate rain forest
Tropical rain forest
Tropical seasonal forest/savanna
Subtropical desert
Temperate grassland/desert
Woodland/shrubland
Termite discovery
Undiscovered
Discovered

Fig. 1

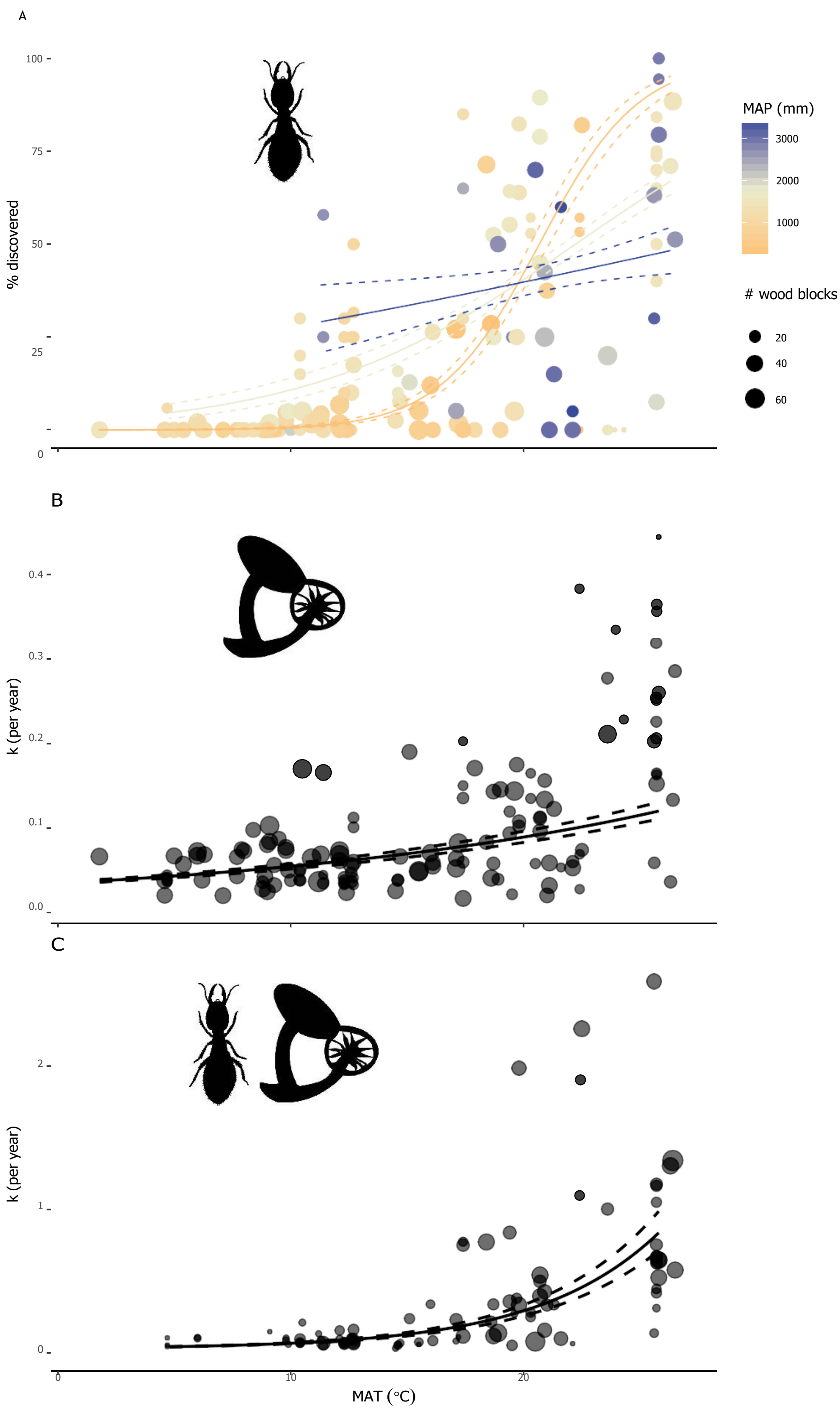

A
% discovered
MAP (mm)
3000
2000
1000
wood blocks
20
40
60
B
k (per year)
C
k (per year)
MAT (°C)

Fig. 2

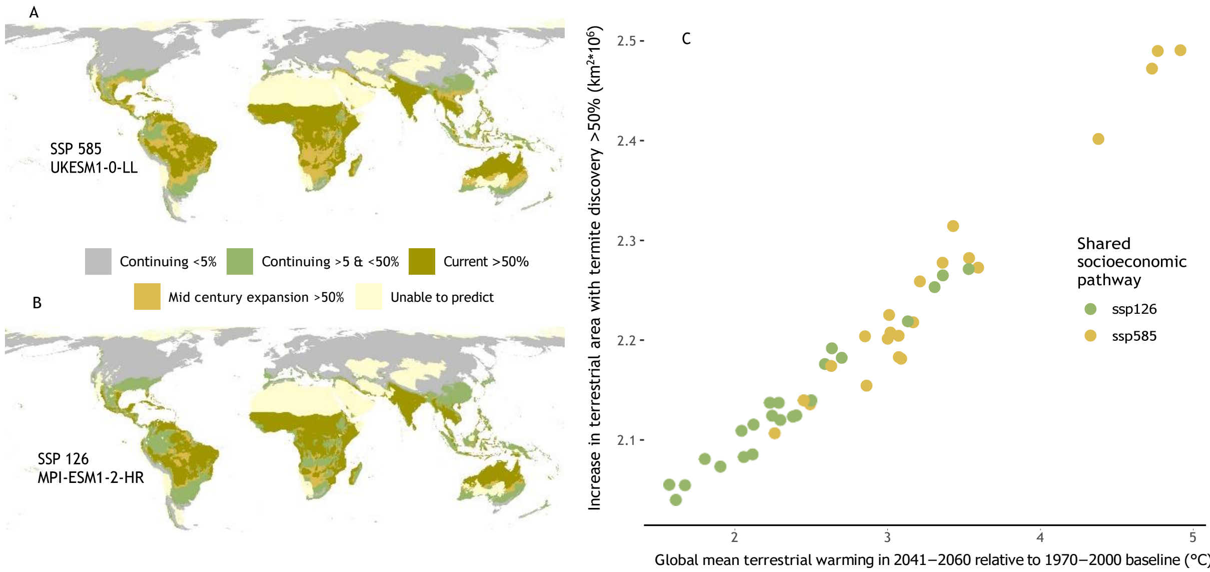
A
SSP 585
UKESM1-0-LL
Continuing <5%
Continuing >5 & <50%
Current >50%
Mid century expansion >50%
Unable to predict
B
SSP 126
MPI-ESM1-2-HR
C
Increase in terrestrial area with termite discovery >50% (km²*10⁶)
2.5
2.4
2.3
2.2
2.1
2
3
4
5
Global mean terrestrial warming in 2041−2060 relative to 1970−2000 baseline (°C)
Shared
socioeconomic
pathway
ssp126
ssp585

Fig. 3

Science
AAAS

Supplementary Materials for

Temperature sensitivity of termites is a major determinant of global wood decay rates

Amy E. Zanne, Habacuc Flores-Moreno, Jeff R. Powell, William K. Cornwell, James W. Dalling, Amy T. Austin, Aimee T. Classen, Paul Eggleton, Kei-ichi Okada, Catherine L. Parr, E. Carol Adair, Stephen Adu-Bredu, Md Azharul Alam, Carolina Alvarez-Garzón , Deborah M.G. Apgaua, Roxana Aragón, Marcelo Ardón, Stefan K. Arndt, Louise A. Ashton, Nicholas A. Barber, Jacques Beauchene, Matty P. Berg, Jason Beringer, Matthias M. Boer, José Antonio Bonet, Katherine Bunney, Tynan J. Burkhardt, Dulcineia de Carvalho, Dennis Castillo-Figueroa, Lucas A. Cernusak, Alexander William Cheesman, Taina M. Cirne-Silva, Jamie Cleverly, Johannes H.C. Cornelissen, Timothy J. Curran, André Mouro D'Angioli, Caroline Dallstream, Nico Eisenhauer, Fidele Evouna Ondo, Alex Fajardo, Romina D. Fernandez, Astrid Ferrer, Marco Aurélio Leite Fontes, Mark L. Galatowitsch, Grizelle González, Felix Gottschall, Peter R. Grace, Elena Granda, Hannah M. Griffiths, Mariana Guerra Lara, Motohiro Hasegawa, Mariet M. Hefting , Nina Hinko-Najera, Lindsay B. Hutley, Jennifer M. Jones, Anja Kahl, Mirko Karan, Joost A. Keuskamp, Tim Lardner, Michael J. Liddell, Craig Macfarlane, Cate Macinnis-Ng, Ravi Fernandes Mariano, M. Soledad Méndez, Wayne S. Meyer, Akira S. Mori, Aloysio Souza de Moura, Matthew Northwood, Romà Ogaya, Rafael S. Oliveira, Alberto Orgiazzi, Juliana Pardo, Guille Peguero, Josep Penuelas, Luis Ignacio Perez, Juan Manuel Posada, Cecilia Margarita Prada, Tomáš Přívětivý, Suzanne M. Prober, Jonathan Prunier, Gabriel Willie Quansah, Víctor Resco de Dios, Ronny Richter, Mark Peter Robertson, Lucas Fernandes Rocha, Megan A. Rúa, Carolina Sarmiento, Richard P. Silberstein , Mateus Cardoso Silva, Flávia Freire Siqueira, Matthew Glenn Stillwagon , Jacqui Stol, Melanie K. Taylor, Francois Philippe Teste, David Yue Phin Tng, David Tucker, Manfred Türke, Michael D. Ulyshen, Oscar J. Valverde-Barrantes, Eduardo van den Berg,Richard S.P. van Logtestijn, G.F. (Ciska) Veen, Jason G. Vogel, Timothy J. Wardlaw, Georg Wiehl, Christian Wirth, Michaela J. Woods, Paul-Camilo Zalamea

Correspondence to: aezanne@gmail.com

This PDF file includes:

Materials and Methods
Figs. S1 to S4
Tables S1 to S12

Materials and Methods

In this study, 8,922 wood blocks were deployed across 133 sites in 20 countries and on all continents except Antarctica (Figure 1A, table S11). The majority of sites were established in 2017, with 6 sites established in 2018 in Puerto Rico with the delay due to Hurricane Maria. Untreated wood was sourced from locations within countries or regions (i.e., Europe) and followed protocols established in Cheesman et al. (*18*). Field sites were all part of individual PI's local projects, meaning they were under the umbrella of ongoing projects, not needing specific permits. Most locations used *Pinus radiata*, but a few study sites were unable to access *P. radiata*; they instead used *P. taeda* (Brazil), *P. elliotti* (French Guiana), or southern yellow pine (likely *P. echinata*) (Panama). We accounted for these differences based on wood chemistry (see below). We targeted wood-dwelling microbes and wood-feeding termites in this study as these are the two primary biotic wood decay agents globally (*7*). We note that this study uses a common substrate, allowing us to leverage a network of climatically diverse sites to directly compare differences in decay agents and environmental gradients. This is a logical first step to address such questions; however, using targeted pine wood from sawn lumber has limitations. It lacks bark and may interact with local decay agents differently to native species that vary in wood construction to pine.

Wood was cut into blocks at volume of ~403 cm^3 and blocks were dried at 120°C to constant mass and weighed for initial dry mass. Wood blocks were haphazardly divided into two treatments; all treatments allowed wood-dwelling microbe access with half the blocks excluding (=microbes) and the other half including (=microbes+termites) wood-feeding termites. Wood blocks in all treatments were wrapped with 300 **μ**m nylon or polyester mesh bags sealed with stainless-steel staples. Bags in the microbes+termites treatment had 10 holes (~5 mm diameter) punched into the mesh on the underside of the mesh bag to allow termite access. In our statistical analyses (see below), holes did not alter wood decay rates e.g., through altered microclimate.

Sites deployed 20 stations (with a few deploying less); each station had treatment pairs of wood blocks, one for microbes and one for microbes+termites. Treatment pairs were replicated at each station for all planned harvest time points (table S11), and one treatment pair was removed from each station at a given harvest time point. All sites had harvests at ~12 months and most sites had harvests at ~24 months with some sites including ~6 month, ~36 month and/or ~48 month harvests (table S11). Stations were spaced $\geq$5 m apart from one another and $\geq$0.5m away from existing large deadwood, termite mounds, exposed rocks or substantial water flow paths. All wood blocks were covered with 70% green shade cloth to reduce solar radiation degradation of mesh bags.

For initial wood samples from each source location, 3-5 blocks were sent to University of Illinois for analysis. Sawdust samples from individual blocks were ground and analyzed for % nitrogen and % carbon content using an elemental analyzer (Costech, Valencia, CA, USA) (table S11). Average elemental % nitrogen and % carbon per source location were used to represent variation within and across wood species as wood chemistry typically is a strong predictor of decay rates (*25*, *26*) (tables S6-10).

Wood blocks were randomly selected from each treatment at each station for harvest at ~6 months (n = 777, sites = 22), ~12 months (n = 4479, sites = 120), ~24 months (n = 3487, sites = 96), ~36 months (n = 125, sites = 10) and ~48 months (n = 54, sites = 10) after deployment. Once collected, wood blocks were assessed for termites. We determined termite discovery and decay following a two-step method. First, we filtered to those sites where site researchers recorded termite presence. Second, for those sites with termites, we recorded blocks as discovered when they were noted as having termites, mudding (i.e., imported soil), and/or damage (e.g., internal chambering, external surface scoring, or removal) in wood blocks (fig. S3). When wood blocks were observed to be damaged, but this damage was not attributable to termites (e.g., small holes, non-termite larvae, etc.), these blocks were recorded as undiscovered by termites. Few blocks had macrofauna damage not attributable to termites (termite discovery was 2.3× higher than discovery by other macrofauna). One block was dropped from the study as we were unable to determine its termite discovery status. After termite discovery assessment, wood blocks were cleaned, separating out deadwood from imported soil, termites, fungal fruiting bodies, roots, etc. and dried at 100°C for 72 hrs before reweighing for final mass.

Using site latitude and longitude, we obtained elevation (m) and climate variables from Fick and Hijmans (*27*), including both mean annual temperature (MAT; °C) and mean annual precipitation (MAP; mm) at 0.5° resolution; climate data were summarized over the window over which the blocks were deployed at field sites. We selected MAT and MAP to capture the broad climate envelope at our sites (as opposed limits such as minimum or maximum) as our goals were to examine climate sensitivities of wood-dwelling microbes and wood-feeding termites, which are typically compared under climate averages (e.g., Q_{10}). Whittaker's biomes were obtained from Ricklefs (*24*). We used "raster" (*28*) and "plotbiomes" (*29*) packages in R (v4.04) (*30*).

Analyses *Discovery* - Termite discovery was calculated as the estimated percentage of wood blocks at all sites per year in the microbes+termites treatment that were noted as having termites. We ran two sets of two-tailed analyses to understand how wood block discovery by termites varied across geographic and climatic space. First, we ran a series of bivariate logistic regressions (using the glm function in R (*30*)), examining how individual spatial (Absolute (Latitude) and elevation) and climatic (MAT and MAP) predictors estimated discovery. Second, we ran a multivariate logistic regression (using the glm function in R (*30*)) including MAT, MAP and their interaction to estimate discovery. In both models, we estimated termite discovery at the block level using all wood blocks in the microbe+termite treatment (discovered or undiscovered) per site and used an offset for time since deployment to account for variation in deployment length. While no site occurred where *P. radiata* is native, 43 of the sites occurred where other *Pinus* spp. were native. To check that exposure to native species within the *Pinus* genus did not lead to increased decay rates, we included *Pinus* presence as a term in the multivariate models. *Pinus* presence was not a significant term in either model and we excluded it from further analyses.

Decay - We calculated proportion mass loss (ML) for a given time window = 1 - (Initial mass - Final mass/ (Initial mass * Time)). Microbial-driven (M) wood ML was calculated for blocks undiscovered by termites, while microbial and termite-driven (M+T) wood ML was calculated for blocks discovered by termites. Additionally, decay was calculated as average decay per discovery category at a site assuming an exponential steady-state of decay using percentage mass loss and time since deployment (i.e., k = -log (Final mass/Initial mass)/time). We averaged decay by discovery category and site and applied a natural-log transformation prior to analyses. Data were weighted such that those decay per discovery categories and sites with higher sample sizes (i.e., number of wood blocks) were given greater weight in the regression. Similar to the discovery models, we ran two sets of two-tailed analyses to understand how both termite undiscovered and discovered decay rates (ln(k)) varied across geographic and climatic space. First, we ran a series of bivariate regressions (using the lm function in R (*30*)), examining how individual spatial (Absolute (Latitude) and elevation) and climatic (MAT and MAP) predictors estimated k for discovered and undiscovered wood categories. Second, we ran a multivariate regression including MAT, MAP and their interaction (using the lm function in R

(*30*)) to estimate decay for each discovered and undiscovered wood category. We also ran a third analysis to confirm the relationship between the magnitude of discovery and decay. For this analysis, we confirmed that decay rates increased with more frequent discovery by termites in a biome-specific fashion (Fig. S4) by regressing decay rates against the percentage of wood blocks discovered at each site, the biome associated with each site and the interaction between discovery and biome (using the lm and Anova functions in R (*30*)). In discovery and decay models, when we included initial wood % nitrogen and % carbon to account for pine species, both variables were significant but otherwise had little effect on models (tables S6-10); weak effects of latitude and precipitation became not significant in M (termite undiscovered) decay models (tables S2, 7). Holes in the mesh did not alter decay rates (e.g., due to altered microclimate) when we analyzed the effect of hole treatment (holes/no holes) using a two-tailed test for all blocks undiscovered by termites (main effect and all interactions involving that treatment $P > 0.4$). For analyses, we used the "lubridate" (*31*), "boot" (*32*), "report" (*33*), "see" (*34*), "correlation" (*35*), "modelbased" (*36*), "effectsize" (*37*), "parameters" (*38*), "performance" (*39*), "bayestestR" (*40*), "datawizard" (*41*), "insight" (*42*), "easystats" (*43*), "lme4" (*44*), "patchwork" (*45*), "ggeffects" (*46*), "forcats" (*47*), "stringr" (*48*), "dplyr" (*49*), "purrr" (*50*), "readr" (*51*), "tidyr" (*52*), "tibble" (*53*), "ggplot2" (*54*), "tidyverse" (*55*), "*khroma*" (*56*) and "*car*" (*57*) packages in R (v4.04) (*30*).

Fixed- versus mixed-effects models - We assumed that geographic signatures in spatial and climate variables would already account for variation associated with "site". Further, including "site" in models would make it difficult to estimate coefficients associated with climate variables; we modeled discovery and decay without explicitly accounting for multiple wood blocks and harvests associated with each "site". To confirm that outcomes of statistical hypothesis tests were robust to this decision, we also fit mixed effects models (using lmer and glmer functions from "lme4" (*44*)) including each "site" as a random effect (Table S12).

Termite discovery land surface area estimations - To explore amount of land surface area potentially impacted by high termite discovery (assuming all else as equal, e.g., we did not model how climate change alters vegetation distributions, land surface area due to sea level rise, or termite or microbial decay rates), we first estimated from our model where high termite discovery (>50%) should be expected based on MAT and MAP macroclimate relationships from our data (Table S3). To bracket how climate change may lead to spatial shifts in termite discovery by mid-century, we estimated land area predicted to have high discovery by 2041-2060 based on all available mid-century CMIP6 climate models for scenarios SSP 5-8.5 or SSP 1-2.6 downscaled to 2.5 minute resolution and bias corrected using WorldClim v2.1 (*27*). Finally, we estimated percentage land area that has only rare termite discovery (<5%), currently has low and is not expected to have high discovery (>5% & <50%) and are warm sites (either now or in mid-century) that are drier or wetter than any sites in the current study by $\pm$ 10%, meaning we were unable to predict termite discovery rates. Here, we focus on areas that currently have <50% discovery but are expected to expand to >50% discovery by mid-century. The 50% discovery threshold is arbitrary, but we selected it as it is both a biologically useful part of climate-termite discovery relationships and statistically robust. Focusing on a 50% threshold is analogous to common approaches in many other fields (e.g., median lethal dose, LD_{50}).

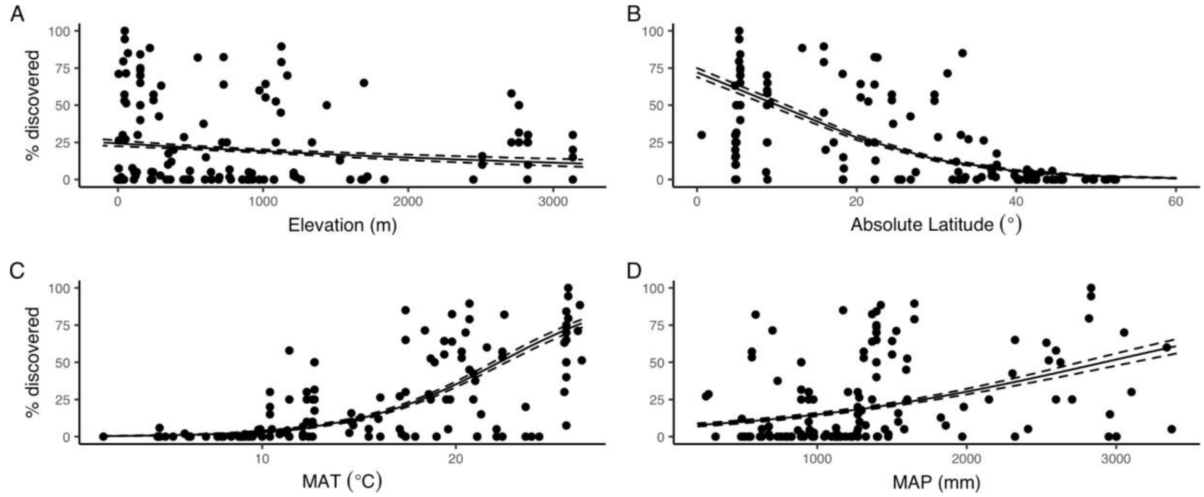

Fig. S1.

Termite discovery versus key spatial and climatic variables: (A) Elevation, (B) Absolute (Latitude), (C) Mean annual temperature (MAT), and (D) and Mean annual precipitation (MAP). We ran logistic regressions with individual spatial and climatic variables as predictors of probability of wood block discovery with an offset for time since deployment. The solid black line is the model best fit and dashed line is the 95% CI (table S1). Termite discovery was estimated at the block level using all wood blocks in the microbe+termite treatment (discovered or undiscovered) per site. Each circle represents the estimated percentage of wood blocks with evidence of termites per year at a site. Median termite discovery = 10%; 95th percentile = 82%.

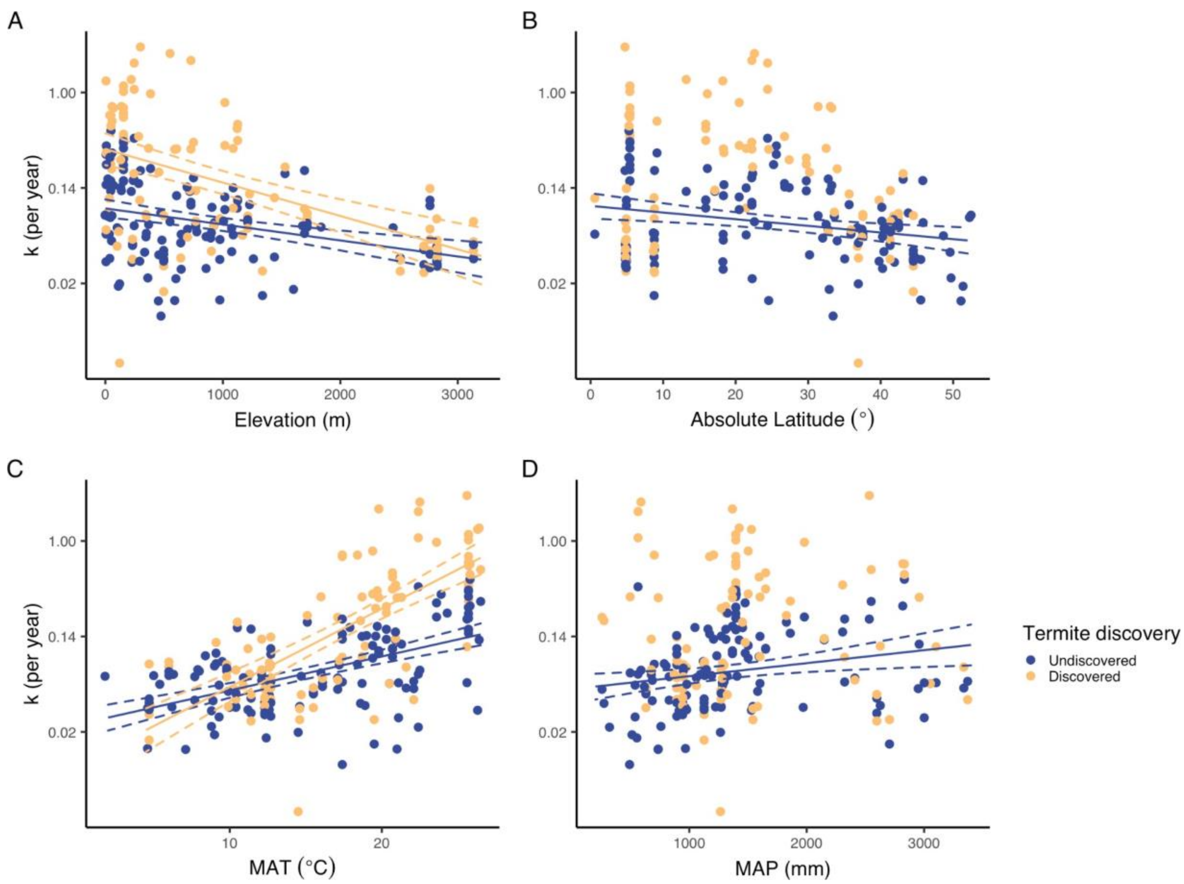

Fig. S2.

Microbe (termite undiscovered) and microbe + termite (termite discovered) decay (k) versus key spatial and climatic variables: (**A**) Elevation, (**B**) (Absolute) Latitude, (**C**) Mean annual temperature (MAT), and (**D**) and Mean annual precipitation (MAP). Note that the y-axis is ln-transformed but tick labels represent untransformed values for decay. We ran linear regressions with individual spatial and climatic variables as predictors of decay rates (k) separately for termite discovered and undiscovered wood categories. Blue lines denote termite undiscovered wood blocks and orange lines denote termite discovered wood blocks. The solid lines are the model best fit and dashed lines are the 95% CI (tables S2-3). There were no significant relationships between termite discovered decay and either (Absolute) Latitude (**B**) or MAP (**D**). Median termite undiscovered wood mass loss in two years = 11% (95th percentile = 43%), and median estimated termite discovered wood mass loss in two years = 23% (95th percentile = 92%).

Fig. S3.

Examples of decayed wood blocks. (A) Termite discovered wood from 'Gingin' (Western Australia) after 488 days of exposure. (**B**) Microbes wood undiscovered by termites from the same harvest as the pair of blocks shown in (**A**) for comparison. (**C**) Termite discovered wood from Australia savanna from the pilot study after 339 days of exposure. (**D**) The same block shown in C with wood (upper left) and imported soil (right).

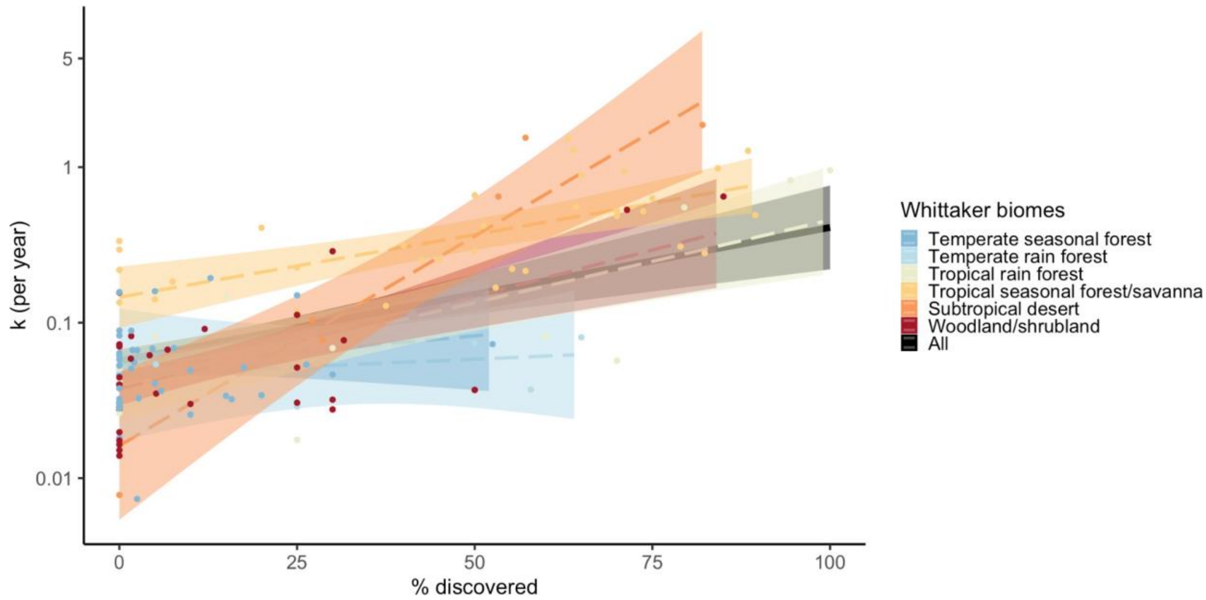

Fig. S4.
Relationship between discovery and decay (k) of wood blocks. Note that the y-axis is ln-transformed but tick labels represent untransformed values for decay. Decay increased exponentially at sites as the percentage of wood blocks discovered by termites increased ($ANOVA_{discovery}$: $F_{1,119} = 77.1$, $P < 0.001$), as shown by the black line (+/- 95% CI). The rate of increase differed among biomes ($ANOVA_{discovery:biome}$: $F_{5,119} = 3.5$, $P = 0.005$), with the steepest slope for subtropical deserts and the shallowest slope for temperate rain forest. The analysis is limited to biomes for which there were at least six sites with termite discovery.

Table S1.
Best fit bivariate models for termite discovery versus key spatial and climatic variables: Elevation, Absolute (Latitude), Mean annual temperature (MAT), and Mean annual precipitation (MAP), including Parameter (Par), Odds Ratio, SE, 95% CI, z-scores, P values and McFadden's pseudo-R^2, (DF = 4465, N = 4466). We ran logistic regressions with individual spatial and climatic variables as predictors of probability of wood block discovery with an offset for time since deployment. Termite discovery was estimated at the block level using all wood blocks in the microbe+termite treatment (discovered or undiscovered) per site. Significant parameters are in bold.

Par	Odds Ratio	SE	95% CI	*z*	*P*	pseudo-R^2
Model						**0.229**
Intercept	**0.62**	**0.05**	**(0.53, 0.72)**	**-6.34**	**< 0.001**	
Absolute Latitude	**0.91**	**2.82E-03**	**(0.90, 0.92)**	**-30.32**	**< 0.001**	
Model						**0.007**
Intercept	**0.08**	**4.10E-03**	**(0.07, 0.09)**	**-48.02**	**< 0.001**	
Elevation	**1**	**5.11E-05**	**(1.00, 1.00)**	**-5.99**	**< 0.001**	
Model						**0.290**
Intercept	**5.48E-04**	**9.38E-05**	**(0, 0)**	**-43.88**	**< 0.001**	
MAT	**1.31**	**0.01**	**(1.29, 1.34)**	**31.64**	**< 0.001**	
Model						**0.063**
Intercept	**0.02**	**1.43E-03**	**(0.01, 0.02)**	**-48.18**	**< 0.001**	
MAP	**1**	**5.04E-05**	**(1.00, 1.00)**	**18.06**	**< 0.001**	

Table S2.
Best fit bivariate models for decay (ln(k)) versus key spatial and climatic variables: Elevation, Absolute (Latitude), Mean annual temperature (MAT), and Mean annual precipitation (MAP), including Termite discovery (Dis; Termite undiscovered wood blocks (M), Termite discovered wood blocks (M+T)), Parameter (Par), Coefficient (Coef), SE, 95% CI, z-score, P values and Adjusted-R^2 (DF = 221, N = 225). We ran linear regressions with individual spatial and climatic variables as predictors of decay rates (k) separately for termite discovered and undiscovered wood categories. Decay was estimated as the exponential rate of decay per year and was averaged by site and natural-log transformed prior to analysis. Significant parameters are in bold.

Dis	Par	Coef	SE	95% CI	*t*	*df*	*P*	R^2 (Adj)
Model								0.021
M+T	**Intercept**	**-1.51**	**0.25**	**(-1.99, -1.02)**	**-6.12**	**91**	**< 0.001**	
	Latitude	-0.02	9.87E-03	(-0.04, 0)	-1.73	91	0.087	
Model								**0.060**
M	**Intercept**	**-2.38**	**0.14**	**(-2.64, -2.11)**	**-17.48**	**130**	**< 0.001**	
	Latitude	**-0.01**	**4.54E-03**	**(-0.02, 0)**	**-3.07**	**130**	**0.003**	
Model								**0.253**
M+T	**Intercept**	**-1.19**	**0.17**	**(-1.53, -0.85)**	**-7.01**	**91**	**< 0.001**	
	Elevation	**-6.99E-04**	**1.23E-04**	**(0, 0)**	**-5.67**	**91**	**< 0.001**	
Model								0.128
M	**Intercept**	**-2.43**	**0.1**	**(-2.62, -2.24)**	**-25.38**	**130**	**< 0.001**	
	Elevation	**-3.35E-04**	**7.46E-05**	**(0, 0)**	**-4.49**	**130**	**< 0.001**	
Model								**0.521**
M+T	**Intercept**	**-4.7**	**0.3**	**(-5.29, -4.10)**	**-15.7**	**91**	**< 0.001**	
	MAT	**0.16**	**0.02**	**(0.13, 0.20)**	**10.06**	**91**	**< 0.001**	
Model								**0.310**

M	**Intercept**	**-3.84**	**0.16**	**(-4.15, -3.53)**	**-24.72**	**130**	**< 0.001**	
	MAT	**0.07**	**9.18E-03**	**(0.05, 0.09)**	**7.75**	**130**	**< 0.001**	
Model								-0.010
M+T	**Intercept**	**-1.93**	**0.33**	**(-2.58, -1.28)**	**-5.86**	**91**	**< 0.001**	
	MAP	5.07E-05	2.01E-04	(0, 0)	0.25	91	0.801	
Model								**0.045**
M	**Intercept**	**-3.1**	**0.16**	**(-3.41, -2.80)**	**-19.95**	**130**	**< 0.001**	
	MAP	**2.72E-04**	**1.01E-04**	**(<-0.0001, <0.0001)**	**2.69**	**130**	**0.008**	

Table S3.
Best fit multivariate model for probably of termite discovery versus climatic sensitivities: Mean annual temperature (MAT) and Mean annual precipitation (MAP), including Parameter (Par), Odds Ratio, SE, 95% CI, z-scores, P values (McFadden's pseudo-R^2 = 0.31, DF = 4462, N = 4466). We ran a multivariate logistic binomial regression including MAT, MAP and their interaction as predictors of probability of wood block discovery with an offset for time since deployment. Termite discovery was estimated at the block level using all wood blocks in the microbe+termite treatment (discovered or undiscovered) per site. Significant parameters are in bold.

Par	Odds Ratio	SE	95% CI	*z*	*P*
Intercept	**6.32E-06**	**2.94E-06**	**(2.52E-06, 1.56E-05)**	**-25.76**	**< 0.001**
MAP	**1**	**3.13E-04**	**(1.00, 1.00)**	**10.73**	**< 0.001**
MAT	**1.67**	**0.04**	**(1.59, 1.75)**	**21.21**	**< 0.001**
MAP × MAT	**1**	**1.52E-05**	**(1.00, 1.00)**	**-11.17**	**< 0.001**

Table S4.
Best fit multivariate model for microbe (termite undiscovered) wood decay (ln(k)) versus climatic sensitivities: Mean annual temperature (MAT) and Mean annual precipitation (MAP), including Parameter (Par), Coefficient (Coef), SE, t-values and P values (R^2 = 0.214, DF = 128, N = 132). We ran a multivariate linear regression including MAT, MAP and their interaction for the undiscovered wood category. Significant parameters are in bold. Decay was estimated as the exponential rate of decay per year and was averaged by site and natural-log transformed prior to analysis.

Par	Coef	SE	*t*	*P*
Intercept	**-4.38**	**0.48**	**-9.12**	**< 0.001**
MAT	**0.09**	**0.03**	**3.18**	**0.002**
MAP	0.73	0.40	1.82	0.072
MAT × MAP	-0.03	0.02	-1.55	0.124

Table S5.

Best fit multivariate model for microbe + termite (termite discovered) wood decay (ln(k)) versus climatic sensitivities: Mean annual temperature (MAT) and Mean annual precipitation (MAP), including Parameter (Par), Coefficient (Coef), SE, t-values and P values (R^2 = 0.69, DF = 89, N = 93) We ran a multivariate linear regression including MAT, MAP and their interaction for the discovered wood category. Significant parameters are in bold. Decay was estimated per year, averaged by site and natural-log transformed prior to analyses.

Par	Coef	SE	*t*	*P*
Intercept	**-4.97**	**0.78**	**-6.35**	**< 0.001**
MAT	**0.24**	**0.04**	**6.12**	**< 0.001**
MAP	-0.55	0.49	-1.13	0.260
MAT × MAP	-0.007	0.02	-0.31	0.755

Table S6.

Best fit bivariate models for termite discovery versus key spatial and climatic variables and wood chemistry: Mean annual temperature (MAT), Mean annual precipitation (MAP), % nitrogen (%N) and % carbon (%C), including Parameter (Par), Odds Ratio, SE, 95% CI, z-scores, P values and McFadden's pseudo-R^2, (DF = 4465, N = 4466). We ran logistic regressions with individual spatial and climatic variables, as well as %N and %C, as predictors of probability of block discovery with an offset for time since deployment. Termite discovery was estimated at the block level using all wood blocks in the microbe+termite treatment (discovered or undiscovered) per site. Significant parameters are in bold.

Par	Odds Ratio	SE	95% CI	*z*	*P*	pseudo-R^2
Model						
Intercept	**7.00E-28**	**2.26E-27**	**(0, 0)**	**-19.39**	**< 0.001**	**0.311**
Absolute Latitude	**0.93**	**3.13E-03**	**(0.92, 0.94)**	**-21.62**	**< 0.001**	
%N	**1.77E+09**	**2.46E+09**	**(1.18E+08, 2.76E+10)**	**15.31**	**< 0.001**	
%C	**3.28**	**0.20**	**(2.91, 3.71)**	**19.09**	**< 0.001**	
Model						
Intercept	**4.18E-42**	**1.35E-41**	**(0, 0)**	**-29.45**	**< 0.001**	**0.215**
Elevation	**1**	**5.86E-05**	**(1.00, 1.00)**	**4.08**	**< 0.001**	
%N	**2.73E+14**	**3.98E+14**	**(1.61E+13, 4.86E+15)**	**22.82**	**< 0.001**	
%C	**5.91**	**0.37**	**(5.24, 6.69)**	**28.52**	**< 0.001**	
Model						
Intercept	**1.20E-20**	**4.08E-20**	**(0, 0)**	**-13.43**	**< 0.001**	**0.318**
MAT	**1.23**	**0.01**	**(1.21, 1.26)**	**21.32**	**< 0.001**	
%N	**1.91E+06**	**2.93E+06**	**(9.754E+04, 3.96E+07)**	**9.44**	**< 0.001**	
%C	**2.14**	**0.14**	**(1.87, 2.44)**	**11.20**	**< 0.001**	
Model						
Intercept	**2.08E-38**	**6.37E-38**	**(0, 0)**	**-28.29**	**< 0.001**	**0.223**

MAP	**1**	**6.44E-05**	**(1.00, 1.00)**	**7.57**	**< 0.001**
%N	**1.80E+12**	**2.75E+12**	**(9.29E+10, 3.71E+13)**	**18.47**	**< 0.001**
%C	**5.01**	**0.30**	**(4.46, 5.63)**	**27.21**	**< 0.001**

Table S7.
Best fit bivariate models for decay (ln(k)) versus key spatial versus climatic variables and wood chemistry: Elevation, Absolute (Latitude), Mean annual temperature (MAT), Mean annual precipitation (MAP), % nitrogen (%N) and % carbon (%C), including Termite discovery (Dis; Termite undiscovered wood blocks (M), Termite discovered wood blocks (M+T)), Parameter (Par), Coefficient (Coef), SE, 95% CI, z-score, P values and Adjusted-R^2 (DF = 217, N = 225). We ran linear regressions with individual spatial and climatic variables, as well as %N and %C, as predictors of decay rates (k) separately for termite discovered and undiscovered wood categories. Decay was estimated as the exponential rate of decay per year and was averaged by site and natural-log transformed prior to analysis. Significant parameters are in bold.

Dis	Par	Coef	SE	95% CI	*t*	*df*	*P*	R^2 (Adj)
Model								
M+T	**Intercept**	**-52.33**	**7.11**	**(-66.45, -38.21)**	**-7.36**	**89**	**< 0.001**	**0.368**
	Absolute Latitude	3.03E-03	8.46E-03	(-0.01, 0.02)	0.36	89	0.721	
	%N	**13.51**	**2.93**	**(7.68, 19.34)**	**4.6**	**89**	**< 0.001**	
	%C	**0.99**	**0.14**	**(0.71, 1.26)**	**7.08**	**89**	**< 0.001**	
Model								
M	**Intercept**	**-28.51**	**4.51**	**(-37.43, -19.59)**	**-6.32**	**128**	**< 0.001**	**0.251**
	Absolute Latitude	-3.17E-03	4.45E-03	(-0.01, 0.01)	-0.71	128	0.478	
	%N	**9.19**	**1.87**	**(5.48, 12.89)**	**4.9**	**128**	**< 0.001**	
	%C	**0.5**	**0.09**	**(0.33, 0.67)**	**5.71**	**128**	**< 0.001**	
Model								
M+T	**Intercept**	**-40.67**	**7.13**	**(-54.83, -26.50)**	**-5.7**	**89**	**< 0.001**	**0.435**
	Elevation	**-3.94E-04**	**1.20E-04**	**(0, 0)**	**-3.28**	**89**	**0.001**	
	%N	**10.47**	**2.78**	**(4.95, 15.99)**	**3.77**	**89**	**< 0.001**	
	%C	**0.77**	**0.14**	**(0.49, 1.04)**	**5.47**	**89**	**< 0.001**	
Model								
M	**Intercept**	**-25.71**	**4.24**	**(-34.09, -17.33)**	**-6.07**	**128**	**< 0.001**	**0.291**

	Elevation	**-1.99E-04**	**7.16E-05**	**(0, 0)**	**-2.78**	**128**	**0.006**	
	%N	**8.38**	**1.79**	**(4.85, 11.92)**	**4.69**	**128**	**< 0.001**	
	%C	**0.45**	**0.08**	**(0.28, 0.61)**	**5.4**	**128**	**< 0.001**	
Model								
M+T	**Intercept**	**-24.08**	**7.18**	**(-38.35, -9.82)**	**-3.35**	**89**	**0.001**	**0.555**
	MAT	**0.13**	**0.02**	**(0.09, 0.17)**	**6.12**	**89**	**< 0.001**	
	%N	2.76	2.91	(-3.01, 8.54)	0.95	89	0.344	
	%C	**0.4**	**0.15**	**(0.11, 0.69)**	**2.76**	**89**	**0.007**	
Model								
M	**Intercept**	**-17.93**	**4.66**	**(-27.15, -8.71)**	**-3.85**	**128**	**< 0.001**	**0.348**
	MAT	**0.05**	**0.01**	**(0.03, 0.07)**	**4.43**	**128**	**< 0.001**	
	%N	**5.16**	**1.94**	**(1.32, 9.00)**	**2.66**	**128**	**0.009**	
	%C	**0.28**	**0.09**	**(0.09, 0.46)**	**2.99**	**128**	**0.003**	
Model								
M+T	**Intercept**	**-52.64**	**6.62**	**(-65.80, -39.48)**	**-7.95**	**89**	**< 0.001**	**0.387**
	MAP	-3.52E-04	2.06E-04	(0, 0)	-1.71	89	0.091	
	%N	**17**	**3.55**	**(9.96, 24.05)**	**4.79**	**89**	**< 0.001**	
	%C	**0.99**	**0.13**	**(0.73, 1.25)**	**7.55**	**89**	**< 0.001**	
Model								
M	**Intercept**	**-28.92**	**4.18**	**(-37.19, -20.64)**	**-6.92**	**128**	**< 0.001**	**0.254**
	MAP	9.76E-05	9.87E-05	(0, 0)	0.99	128	0.325	
	%N	**8.79**	**1.96**	**(4.92, 12.66)**	**4.49**	**128**	**< 0.001**	
	%C	**0.5**	**0.08**	**(0.34, 0.67)**	**6.14**	**128**	**< 0.001**	

Table S8.

Best fit multivariate model for probably of termite discovery versus climatic sensitivities and wood chemistry: Mean annual temperature (MAT), Mean annual precipitation (MAP), % nitrogen (%N) and % carbon (%C) including Parameter (Par), Odds Ratio, SE, 95% CI, z-scores, P values (McFadden's pseudo-R^2 = 0.34, DF = 4460, N = 4466). We ran a multivariate logistic binomial regression including MAT, MAP and their interaction, as well as %N and %C, as predictors of probability of block discovery with an offset for time since deployment. Termite discovery was estimated at the block level using all wood blocks in the microbe+termite treatment (discovered or undiscovered) per site. Significant parameters are in bold.

Par	Odds Ratio	SE	95% CI	*z*	*P*
Intercept	**9.25E-21**	**2.93E-20**	**(1.77E-23, 4.35E-18)**	**-14.57**	**< 0.001**
MAP	**1**	**3.14E-04**	**(1.00, 1.00)**	**10.95**	**< 0.001**
MAT	**1.59**	**0.04**	**(1.51, 1.67)**	**18.26**	**< 0.001**
%N	**1.20E+06**	**1.68E+06**	**(7.89E+04, 1.93E+07)**	**9.98**	**< 0.001**
%C	**1.95**	**0.12**	**(1.73, 2.21)**	**10.58**	**< 0.001**
MAP × MAT	**1**	**1.55E-05**	**(1.00, 1.00)**	**-11.4**	**< 0.001**

Table S9.
Best fit multivariate model for microbe (termite undiscovered) wood decay (ln(k)) versus climatic sensitivities and wood chemistry: Mean annual temperature (MAT), Mean annual precipitation (MAP), % nitrogen (%N) and % carbon (%C), including Parameter (Par), Coefficient (Coef), SE, t-values and P values (R^2 = 0.245, DF = 126, N = 132). We ran a multivariate linear regression including MAT, MAP and their interaction, as well as %N and %C, for the undiscovered wood category. Decay was estimated as the exponential rate of decay per year and was averaged by site and natural-log transformed prior to analysis. Significant parameters are in bold.

Par	Coef	SE	*t*	*P*
Intercept	**-17.08**	**5.26**	**-3.25**	**0.002**
MAT	**0.07**	**0.03**	**2.58**	**0.011**
MAP	0.68	0.4	1.71	0.09
%N	**5.84**	**2.2**	**2.65**	**0.009**
%C	**0.25**	**0.1**	**2.35**	**0.021**
MAT × MAP	-0.03	0.02	-1.5	0.136

Table S10.
Best fit multivariate model for microbe + termite (termite discovered) wood decay (ln(k)) versus climatic sensitivities and wood chemistry: Mean annual temperature (MAT), Mean annual precipitation (MAP), % nitrogen (%N) and % carbon (%C), including Parameter (Par), Coefficient (Coef), SE, t-values and P values (R^2 = 0.70, DF = 87, N = 93). We ran a multivariate linear regression including MAT, MAP and their interaction, as well as %N and %C, for the discovered wood category. Decay was estimated as the exponential rate of decay per year and was averaged by site and natural-log transformed prior to analysis. Significant parameters are in bold.

Par	Coef	SE	*t*	*P*
Intercept	**-14.42**	**5.03**	**-2.87**	**0.005**
MAT	**0.24**	**0.04**	**6.23**	**< 0.001**
MAP	-0.43	0.51	-0.84	0.405
%N	**5.17**	**2.31**	**2.24**	**0.028**
%C	0.18	0.1	1.8	0.075
MAT × MAP	-0.02	0.02	-0.85	0.400

Table S11.
Description of study sites. Information on each site is provided including location (country, subregion, biome, latitude, longitude), attributes of deployed blocks (date of deployment, type of wood used, initial nitrogen and carbon concentrations) and attributes of harvested blocks (number of days exposed, number of blocks harvested, percent discovered by termites, average and standard deviation [SD] for the decay constant [k] associated with microbial decay or combined termite + microbial decay [NA values indicate that decay class was not observed for that harvest]).

(see separate .csv file)

Table S12.
Comparison of fixed-effects and mixed-effects models. Summary of differing statistical hypothesis test outcomes, where present, of models that include only fixed-effects parameters and those that also include site-level random effects. Parameter estimates of all fixed-effects models are presented in Tables S1-S10. To compare parameter estimates across each pair of models, see "MEmodelcomp.html" at the project repository (https://doi.org/10.5281/zenodo.6804781).

Location of table where model(s) presented	Differences observed between fixed- and mixed-effects models, where present
Table S1	Elevation is nonsignificant in the mixed-effects model. Consistent outcomes observed for all of the other three models.
Table S2	Consistent outcomes observed for all eight models.
Table S3	Consistent outcomes observed.
Table S4	Consistent outcomes observed.
Table S5	Consistent outcomes observed.
Table S6	Consistent outcomes observed for all four models.
Table S7	Consistent outcomes observed for all eight models.
Table S8	Consistent outcomes observed.
Table S9	Consistent outcomes observed.
Table S10	%C is marginally significant in the mixed-effects model. Consistent outcomes observed for all other parameters.